WITHDRAWN: High-throughput preclinical screening of CD123 scFv to design 3rd generation of CAR T-cell in the treatment of BPDCN patient

Maxime Fredon
INSERM, UMR1098-RIGHT, Université Bourgogne Franche-Comté
Margaux Poussard
INSERM, UMR1098-RIGHT, Université Bourgogne Franche-Comté
Sabeha Biichle
INSERM, UMR1098-RIGHT, Université Bourgogne Franche-Comté
Francis Bonnefoy
INSERM, UMR1098-RIGHT, Université Bourgogne Franche-Comté
Evan Seffar
INSERM, UMR1098-RIGHT, Université Bourgogne Franche-Comté
Elodie Bôle-Richard
INSERM, UMR1098-RIGHT, Université Bourgogne Franche-Comté
Florian Renosi
INSERM, UMR1098-RIGHT, Université Bourgogne Franche-Comté
Romain Boidot
Centre Georges-François Leclerc, ICMUB UMR CNRS 6302
François Anna
Institut Pasteur
Maria Loustau
Invectys
Julien Caumartin
Invectys
Philippe Saas
INSERM, UMR1098-RIGHT, Université Bourgogne Franche-Comté
Eric Deconinck
INSERM, UMR1098-RIGHT, Université Bourgogne Franche-Comté
Etienne Daguindeau
INSERM, UMR1098-RIGHT, Université Bourgogne Franche-Comté
Xavier Roussel
INSERM, UMR1098-RIGHT, Université Bourgogne Franche-Comté

Olivier Adotevi
INSERM, UMR1098-RIGHT, Université Bourgogne Franche-Comté
Fanny Angelot-Delettre
INSERM, UMR1098-RIGHT, Université Bourgogne Franche-Comté
Jeanne Galaine
INSERM, UMR1098-RIGHT, Université Bourgogne Franche-Comté
Francne Garnache-Ottou
francine.garnache@efs.sante.fr

INSERM, UMR1098-RIGHT, Université Bourgogne Franche-Comté

Research Article

Keywords: scFv, CAR T-cell, CD123, safety, BPDCN

Posted Date: May 18th, 2022

DOI: https://doi.org/10.21203/rs.3.rs-1646566/v1

Additional Declarations: No competing interests reported.

EDITORIAL NOTE:

The full text of this preprint has been withdrawn by the authors while they make corrections to the work. Therefore, the authors do not wish this work to be cited as a reference. Questions should be directed to the corresponding author.

Abstract

Background: Blastic Plasmacytoid Dendritic Cell Neoplasm (BPDCN) is an aggressive malignant hemopathy characterized by constant overexpression of the CD123 antigen on 100% of blasts identifying CD123 as an antigenic target for the development of adoptive cell therapy. Chimeric Antigen Receptor-T (CAR-T) are composed of an extracellular domain consisting of a single-chain fragment variable (scFv) targeting a surface antigen expressed on tumor cells. In view of the low expression of CD123 on hematopoietic stem cells, monocytes and endothelial cells, it is necessary to evaluate and select the CD123 CAR-T allowing the best cytotoxicity differential between leukemic and healthy cells.

Methods: We developed five third-generation CD123 CAR-T by substituting scFv, in order to assess changes in efficacy and on-target/off-tumor side effects. Using various *in vitro* and *in vivo* BPDCN models, we evaluated the functionality on BPDCN and the on-target/off-tumor effect on endothelial cell line, monocytes and hematopoietic stem cell (HSC).

Results: Using Incucyte, we confirmed the low cytotoxicity on endothelial cells. We showed an increase in CD123 expression on endothelial cells, dependent on the activation of CAR-T through cytokine secretion. Evaluated by CFU-GM culture, we show that two CAR-T are less cytotoxic against hematopoietic stem cells and these two CAR-T significantly reduce tumor infiltration and increase overall survival of mice in three *in vivo* BPDCN models. Finally, we demonstrate in bulk RNA-sequencing that the most effective CAR-T in an aggressive BPDCN model, upregulates genes associated with cytotoxicity and activation/exhaustion at day 34, with fewer regulatory signatures

Conclusions: Together, these results emphasize the importance of evaluating different scFv for the development of CAR-T, to select the best one, with high cytotoxicity potential and the best safety profile for clinical development.

Background

Blastic plasmacytoid dendritic cell neoplasm (BPDCN) is a rare and aggressive leukemia derived from plasmacytoid dendritic cell (pDC) precursors [1, 2]. No standard of care is available to treat these patients, except hematopoietic cell transplantation (HCT) in first remission [3–5]. There is a clear, unmet need for BPDCN patient treatment.

In the last 10 years, the development of genetically modified T lymphocytes expressing a chimeric antigen receptor (CAR) specific for tumor cells has revolutionized immunotherapy [6]. The CAR consists of a single chain comprising the variable fragment (scFv) of a monoclonal antibody (mAb), fused to the intracellular signaling domain of CD3ζ, as well as one or more co-stimulation domains (such as CD28, OX40, 4-1BB) [7]. A scFv is the reconstructed antigen-binding portion of a conventional mAb [8] connected to the intracellular part via a linker and hinge domain of varying size. Structural modification of these components can lead to modification of the affinity, intensity of the intracellular signal and *in vivo* functionality [9–13], underlining the importance of considering these elements in CAR-T construction. In

this study, we focus on the impact of the scFv part, which is the first element to come in contact with the antigen, thereby impacting signals in the CAR-T cell.

CD123 is the α transmembrane chain of the Interleukin-3 (IL-3) receptor (IL3Rα), which associates as a heterodimer with the β subunit (CD131) to form the IL-3 high affinity receptor (IL-3R). CD123 is highly expressed by basophils and pDC [14], and at a lower level on a fraction of normal hematopoietic stem cells (HSC) (but not on the most immature $CD34^{+}/CD38^{-}$ HSC[15, 16]), myeloid progenitors, monocytes, eosinophils and myeloid dendritic cells [17]. Apart from hematopoietic cells, only endothelial cells are currently known to express low levels of CD123 [18]. On the other hand, the strong expression of CD123 in 100% of BPDCN and in many other haematological diseases (such as acute myeloid leukemia (AML) [19], acute lymphoblastic leukemia (ALL) [20], Hodgkin lymphoma [21], myelodysplastic syndrome (MDS) [22]) makes it a target of choice to develop immunotherapy. Furthermore, there is evidence that CD123 is a marker of leukemic stem cells in AML.

To be able to eliminate leukemic cells while sparing healthy cells [23–25] is a major point of clinical CAR-T development. Some contradictory data have described the potential “on target, off tumor” effect of CAR-T targeting CD123. Mardiros *et al*. showed strong elimination of AML cells expressing CD123, while sparing the formation of granulocytes, macrophages and erythrocytes [26], whereas Gill *et al*. showed a decrease in megakaryotypes, B-lymphocytes, monocytes and myeloid cells [27]. In an MDS model, Stevens *et al*. showed that CD123 CAR-T targets only the CD123 positive cell populations and does not impact normal HSC [28]. More recently, we demonstrated in a humanized mouse model that CD123 CAR-T exerts little or no cytotoxicity against various subsets of normal cells with low CD123 expression [29]. Low CD123 expression on endothelial cells may induce endothelial damage, and importantly it has been shown that CD123 levels increase in an inflammatory context [30–32] and thus, toxicity on endothelial may be evaluated.

Due to the presence of many CAR on the CAR-T surface, CAR-T is more effective compared to the recombinant antibody approach, even with the same antibody/antigen affinity. Indeed, the minimum number of recognized target antigens required to induce cytotoxicity is much lower with CAR-T [33]. Some studies highlight that the sensitivity to the target antigen can be modulated in order to increase the specificity of the CAR-T for its leukemic target, and to decrease the “on-target/off-tumor” effect[34]. In addition, CAR-T expression and stability at the T cell membrane are affected by the structure of scFv[9] and also by the humanized process applied to scFv and co-stimulatory domains [35]. Although the antibody selected for CAR-T has high affinity for its antigenic target, it has been reported that the fusion of the variable regions of the antibody into a single chain could induce a distortion in their orientation, thus decreasing its constant of association, ultimately reducing CAR-T efficacy [36].

In this study, we investigate the impact of the scFv on the functionality and safety of CD123 CAR-T. Based on our lentiviral construct [29], we generated five CD123 CAR-T by substituting scFv. These five CAR-T were evaluated *in vitro* and *in vivo* in order to select the one(s) yielding the highest differential cytotoxicity between $CD123^{high}$ BPDCN cells and healthy $CD123^{low}$ cells.

Methods And Material

Cell culture

CAL-1 (Dr. Maeda, University of Nagasaki, Japan), Gen2.2 (EFS, Patent N° 0.215.927), Daudi (ATCC® : CCL-213™) and MA9-RAS (Dr. James C. Mulloy, University of Cincinnati College of Medicine, USA) were cultivated in RPMI 1640 media (Roswell Park Memorial Institute, Gibco™, Fisher scientific, USA) supplemented with 10% fetal bovine serum (FBS, Gibco™) and 1% antibiotics (Penicillin-streptomycin, Gibco™). HEK-293T (ATCC® : CRL-11268™) cell line was cultured in DMEM media (Dulbecco's Modified Eagle Medium, Eurobio, France) supplemented with 10% fetal bovine serum and 1% antibiotics. Cell lines were cultured in an incubator at 37°C saturated with water vapor containing 5% $C0_2$. Primary cells from BPDCN patients (DC-2008-713 and DC 2016–2791 collections) were used for amplification of primary cells in NSG-S mice to produce PDX (Primary Derived Xenograft) as previously described [54]. Endothelial cell line HMEC-1 (ATCC® : CRL-3243™) was cultured in EGM™-2 medium (EBM™-2 Basal Medium, Lonza, CC-3156 and EGM™-2 Single Quots™ Supplements, Lonza, CC-4176). Adherent cell line HMEC-1 and HEK-293T were taken from the flask wall using trypsin-EDTA 0.5% (Gibco™) when the confluence of the latter reached 80%. Monocytes and hematopoetic stem cells (CD34) were cultured in X-VIVO™ 15 media (Lonza, Bâle, Switzerland) supplemented with 8% of heat-inactivated human serum (EFS, B/FC) and 1% antibiotics.

CAR-T vector production, T-cell transduction and CAR expression

To produce the five CD123 monoclonal antibodies, mice were immunized with the recombinant protein CD123 (301-R3-025, R&D systems, Minneapolis, USA) by footpad or intraperitoneal administration (Diaclone SA, Besançon, France). We used lymph nodes or splenic B cells to produce hybridomas secreting. We selected Hybridomas based on the affinity and specificity of monoclonal antibodies using patient's primary cells, $CD123^+$ and $CD123^-$ cell lines and normal blood and bone marrow cells. The sequences encoding CD123 CAR, 2A sequence and the selection market (ΔCD19: truncated CD19) were cloned in a pFLAP lentiviral vector.

CD123 CAR-T lentiviral vectors were produced in HEK-293T. We generated five third-generation CAR-T (CAR N°1 to N°5) directed against CD123 using the same backbone [29], composed of the EF1α promoter [37], two co-stimulation domains (CD28/4-1BB), a CD3ζ signaling domain, a selection domain (ΔCD19), with five different scFv domains (EP20190305816 20190621; WO2020EP67303 20200622), each having various affinity for the CD123 antigen (Fig. 1A). To produce CD123 CAR-T, we used peripheral blood mononuclear cells (PBMC) from healthy donors were collected at the French Blood Center (EFS B/FC, Besançon, France) and obtained after written informed consent. PBMC isolated by Ficoll gradient density centrifugation and were activated with CD3/CD28 Dynabeads (Life Technologies, California, USA). Two days later we assessed lentiviral transduction (MOI of 10) in 24 wells plates (spin at 800g, 32°C for 1h). Transduction efficiency was determined by CD19 expression by flow cytometry (FC) and CAR expression

was determined using a biotinylated CD123 protein as previously described [29]. As control, non-transduced T cells (C0) from the same donors were produced.

Functionality of CD123 CAR-T

Effector cells (C0 or CD123 CAR-T) were labeled with Cell Proliferation Dye Proliferation Dye eFluor 450 (Thermo Fisher, Ecublens, Switzerland). Next, we co-cultured CD123 CAR-T with the indicated cell lines or normal cells at a given effector: target ratio (E: T). After co-culture, cells were labeled with 7-AAD (BD Biosciences, New Jersey, USA), anti-human $CD19^{APC}$ (Miltenyi Biotec, Bergish Gladbach, Germany) and anti-human $CD123^{PE-Cy7}$ (Sony Biotechnology, San Jose, USA).

CD123 CAR-T degranulation was monitored by FC using $CD107a^{PE}$ (BD Biosciences, New Jersey, USA) after 6 hours of E: T co-culture. TNF-α and IFN-γ secretion was assessed in the culture supernatant by ELISA according to the manufacturer's protocols (Diaclone, Besançon, France). Membrane lysis was quantified using LDH release assay by bioluminescence. Real-time cytotoxicity was assessed using the Incucyte. The level of CD123 expression on cell lines was determined by FC.

In vivo models

The animal study was performing under Animal care and use protocol at the University of Besançon (Ministry of Higher Education, Research and Innovation, France, 2021-004-OA-12PR). NSG (NOD-*scid* gamma) mice (8–10 weeks old) were used in this study. NSG mice were irradiated and inoculated intravenously with either luciferase expressing CAL-1 cell line (CAL-1-Luc), PDX or Gen2.2 [29]. C0 and CD123 CAR-T were injected intravenously at the indicated day after injection of tumor cells. Tumor uptake was monitored weekly by bioluminescence (bli) measurements for CAL-1-Luc and by blastic quantification in blood samples by FC for PDX and Gen2.2 models [29].

Bulk RNA-Sequencing Analysis

Bulk RNA-Seq reads were aligned using STAR [38] v2.7.9a to GENCODE Human Release 39 (GRCh38.p13) and read count matrix produced with FeatureCounts [39] v2.0.1, both with default parameters. The Bioconductor RNA-seq workflow was followed to detect differential gene expression with DESEQ2 [40] v1.32.0. A total of 19,337 coding genes were analyzed for transcript abundance and poorly expressed genes were eliminated based on the criteria of a maximum read count > 20 for all samples. Data visualization was achieved in R v4.1.1 with Complex Heatmap package v2.11.1 using DESeq 2's regularized-logarithm transformation (rlog) of the count data.

Statistical Analysis

All data are expressed as mean ± standard deviation (SD). Multiple groups were compared with one-way analysis of variance (ANOVA). All statistical analyses were performed with GraphPad Prism7.0. The thresholds for statistical significance were 0.12 (non-significant, ns), 0.033 (*), 0.002 (**), < 0.001 (***).

More detailed descriptions of the experimental methods and analyses are available in supplementary materials and methods.

Results

CD123 CAR-T transduction efficiency

Transduction efficiency of the five CAR-T (CAR N°1 to N°5) was evaluated by the quantification of T cells co-expressing CD3 and CD19 by FC (Fig. 1B). For CAR N°1, N°3, N°4 and N°5, transduction efficiency above 97% was obtained (N°1: 97.1%±1.1% ; N°3: 97.7%±0.9% ; N°4: 98.2%±0.5% ; N°5: 97.2%±0.9%). CAR N°2 achieved lower transduction efficiency at 65.0% ± 6.0% (Fig. 1C). Moreover, transgene expression was stable over time: the expression of ΔCD19 remained at similar levels between day 7 (D7) and day 23 (D23) post transduction **(**Fig. 1D). CAR expression was evaluated by FC using the biotin-conjugated CD123 protein. At D9, the CAR expression was very high, except for CAR N°2 (N°1: 97.1%±0.6% ; N°2: 60.4%±7.2% ; N°3: 98.0%±0.3% ; N°4: 98.0%±0.4% ; N°5: 97.0%±0.9%, C0: 0.0%±0.2%) (Fig. 1E). We have shown the highest and significant intensity of the biotin-conjugated CD123 protein was detected for CAR N°1 (**Figure S1A**). The five CAR-T products had an identical CD4/CD8 ratio at D7 (**Figure S1B, S1C**).

CD123 CAR-T degranulation and cytotoxicity against BPDCN cell lines

To evaluate the specificity of CAR-T antitumor function, degranulation capacity against the BPDCN cell line CAL-1 ($CD123^{+\,high}$) and $CD123^{-}$ Daudi cell line was assessed (**Figure S1D**). After 6 hours of co-culture (E:T = 1:1), CAR N°1, N°3, N°4 and N°5 had the ability to degranulate against CAL-1 (N°1: 62.6% ±3.8%; N°3: 65.8%±2.2%; N°4: 78.8%±0.7%; N°5: 77.6%±3.6%) compared to C0 (3.3%±0.7%). Only CAR N°2 did not have any degranulation activity (4.3%±1.7%) (Fig. 2A, **left**). No degranulation was observed after co-culture with Daudi (N°1: 5.1%±1.8%; N°2: 1.6%±0.1%; N°3: 6.5%±1.8%; N°4: 5.1%±1.6%; N°5: 3.9%±1.0% and C0: 2.9%±1.1%) (Fig. 2A, **right**) reflecting the specificity of CAR N°1, N°3, N°4 and N°5. Next, CAR-T cytotoxicity was evaluated by FC (7-AAD) after 24 hours of co-culture at E:T = 1:1. CAL-1 were successfully eliminated by CAR N°1, N°3, N°4 and N°5 (N°1: 96.1%±5.5%; N°3: 98.6±1.5%; N°4: 97.4% ±3.7%; N°5: 99.3±0.9%) but not by CAR N°2 (12.4%±5.3%) compared to C0 (2.2%±4.5%) (Fig. 2B, **left**). These results were confirmed with BPDCN PDX (**Figure S2B**), Gen2.2 BPDCN cell line (**Figure S2C**) and $CD123^{+}$ MA-9RAS AML cell line (**Figure S2A**). In contrast, no elimination of Daudi was observed (Fig. 2B, **right**). To evaluate the CAR-T efficacy *in vitro*, CAL-1/ CAR-T co-culture at different E:T ratios ranging from 10:1 to 1:10 was performance. Again, CAR N°1, N°4 and N°5 presented cytotoxic capacity, even with inverted ratios (E:T = 1:5 and 1:10) whereas CAR N°2 had low efficacy for an E:T ratio = 1:1 and CAR N°3 for a ratio of 1:5 (Fig. 2C**).**

CD123 CAR-T cytotoxicity against healthy $CD123^{low}$ cells

In view of the low expression of CD123 by HSC, endothelial cells and monocytes, we evaluated the functionality of CAR-T against these healthy cell types. First, HMEC-1 cell line or monocytes were co-

cultured with CAR-T or C0 for 6 hours at an E:T = 1:1 and T cell CD107a expression was evaluated by FC. We showed that CAR N°1, N°3, N°4 and N°5 slightly degranulated in co-culture with HMEC-1 (N°1: 22.4% ±6.9%; N°3: 28.9%±7.8%; N°4: 32.8%±9.6%; N°5: 25.1%±5.0%, n = 3) (Fig. 3A, **left**) without any significant difference between them and with monocytes (N°1: 29.7%±9.4%; N°3: 43.7%±2.5%; N°4: 38.5±5.3%; N°5: 34.7%±4.8%) (Fig. 3A, **right**). Nevertheless, degranulation capacity of CAR-T is lower against HMEC-1 and monocytes than CAL-1 (Fig. 2A, **left**). Thereafter, membrane lysis capacity of CAR-T was evaluated after 24 hours of co-culture with the different cells at an E:T = 1:1 using LDH release assay. CAR N°1, N°3, N°4 and N°5 were cytotoxic against the CAL-1 cell line (C0: 15.2%±6.6%; N°1: 82.0%±10.3%; N°2: 42.1% ±15.4%; N°3: 88.3%±10.6%; N°4: 89.8%±10.9%; N°5: 88.5%±11.7%) (Fig. 3B) but not against Daudi (C0: 10.9%±6.1%; N°1: 6.9%±2.5%; N°2: 7.2%±6.3%; N°3: 13.1%±4.6%; N°4: 7.2%±1.18%; N°5: 12.6%±4.7%) (Fig. 3C). Moreover, CAR-T presented lower cytotoxicity against HMEC-1 (C0: 5.7%±3.0%; N°1: 35.1% ±3.7%; N°2: 8.7%±0.8%; N°3: 31.2%±7.2%; N°4: 20.7%±8.0%; N°5: 24.9%±9.80%) (Fig. 3D) and monocytes (C0: 1.7%±1.5%; N°1: 26.4%±7.3%; N°2: 2.6%±0.8%; N°3: 31.4%±3.3%; N°4: 16.8%±1.6%; N°5: 21.0%±4.9%) (Fig. 3E) than against CAL-1, without any significant difference between the four functional CAR-T.

For the following parts of the study, we did not evaluate CAR N°2 any further due to its low performance.

To confirm the weaker cytotoxicity of CAR-T against endothelial cells than against CAL-1, apoptosis was assessed by real-time microscopy (Incucyte®) for 8 hours at an E:T = 1:1. The Incucyte® system detects the appearance of green fluorescence, which is proportional to cell death. The average integrated intensity (CU/μ^2) enables normalization of the fluorescence intensity to the cell size. After a short contact time of CAR-T with endothelial cells, toxicity is relatively low (C0: 0.65±0.02 CU/μ^2; N°1: 0.97±0.07 CU/μ^2; N°3: 0.68±0.02 CU/μ^2; N°4: 0.74±0.07 CU/μ^2; N°5: 0.80±0.06 CU/μ^2). In contrast, in the same conditions, more than the half of the CAL-1 cells were eliminated (C0: 0.91±0.08 CU/μ^2; N°1: 1.40±0.04 CU/μ^2; N°3: 1.05±0.08 CU/μ^2; N°4: 1.11±0.19 CU/μ^2; N°5: 1.35±0.69 CU/μ^2) (Fig. 3F). CAR N°1 induced a slight increase in cytotoxicity against HMEC than others but also on CAL-1 with CAR N°5.

Impact of IFN-γ and TNF-α secretion by CD123 CAR-T on CD123 expression by endothelial cells

Secretion of IFN-γ and TNF-α by CAR-T was evaluated by ELISA after 24 hours of co-culture with CAL-1, HMEC-1 or Daudi at an E:T = 1:1. All CAR-T produced higher concentrations of IFN-γ (Fig. 4A) and TNF-α (Fig. 4B) after contact with CAL-1 compared to Daudi or HMEC-1. (**Supplemental table 1 and 2**). To assess whether this pro-inflammatory environment could modulate CD123 expression by endothelial cells, we used a Transwell tri-culture model (CAR-T or C0 ± CAL-1 in the upper chamber and HMEC-1 in the lower chamber) (Fig. 4C). After 24 hours of co-culture at an E:T = 1:1, the RFI of CD123 expression on endothelial cells was assessed. Presence of CAR-T alone does not induce an increase in CD123 expression by HMEC-1 (RFI, HMEC-1 alone: 1.16 ± 0.12; C0: 1.02 ± 0.30; N°1: 1.30 ± 0.48; N°3: 1.06 ± 0.40; N°4: 1.20 ± 0.13; N°5: 0.94 ± 0.13). In contrast, incubation of CAR-T with CAL-1 induced a significant increase in CD123 expression by HMEC-1 (RFI: C0 + CAL-1: 1.12 ± 0.14; N°1 + CAL-1: 2.83 ± 0.65; N°3 + CAL-1: 2.85 ± 0.57; N°4 + CAL-1: 2.87 ± 0.33; N°5 + CAL-1: 2.46 ± 0.763) (Fig. 4C). Culturing HMEC-1 with

recombinant IFN-γ and/or TNF-α, with or without their respective inhibitors show, this cytokine induce an increase in CD123 expression on endothelial cells than can be reversed with the inhibitor (Fig. 4D). These data highlight that the toxicity of CAR-T against endothelial cells is related to activation of CAR-T through production of IFN-γ and TNF-α.

No influence of CD123 CAR-T on Hematopoietic stem cell (HSC) and colony-forming ability

The cytotoxic potential of CAR-T was evaluated on autologous CD34 + HSC. HSC from cord blood were co-cultured with autologous CAR-T or C0 at an E:T = 1:1 for 18 hours **(Figure S3**). CAR-T cytotoxicity against HSC was evaluated by FC (7-AAD). CAR N°1 and N°4 had non-significantly lower cytotoxicity then the two others (30.3%±6.7% and 26.2% ± 20.6% respectively), but close to significance for CAR N°3 (41.3%±7.3%, p = 0.07) (Fig. 5A). In parallel, after co-culture, HSC were placed into human methylcellulose complete medium to examine colony formation (CFU-GM). Fourteen days later, CAR N°1 and N°4 were not shown to affect the clonogenic potential of HSC (Fig. 5B) whereas CAR N°3 had a greater impact on CFU-GM (p = 0.06). For the following experiments, CAR N°3 was no longer evaluated.

Anti-tumor efficacy of CD123 CAR-T *in vivo*

The ability of CAR-T to reduce tumor infiltration was evaluated *in vivo* in NSG mice using the luciferase-expressing CAL-1 cell line (CAL-1-Luc) for the three best CAR-T (N°1, N°4 and N°5) (Fig. 6A). Survival of mice almost doubled after injection of all CAR-T compared with C0 injection (33 days for C0, 68 days for CAR N°1, 59 days for CAR N°4 and 56 days for CAR N°5; 4 mice/group) without a significant difference between the three CAR-T, albeit almost significant for CAR N°5 (p = 0.08), which appeared to perform less well (Fig. 6B). As luminescence reflects the infiltration of leukemia, we followed the tumor load by bioluminescence imaging. Mice treated with CAR-T show a delay in systemic leukemia, without any difference between the three CAR-T (Fig. 6C). We confirmed these data using a BPDCN PDX model (Fig. 6A**)**. At D63 after injection, BPDCN cells ($hCD45^{+}/CD123^{high}$) were detected in blood samples from mice. One group received an IV injection of 5.10^{6} C0 and the three others received 5.10^{6} of CAR-T. The survival of the mice increased significantly after treatment with CAR-T compared to C0 (67 days for C0; 157 days for CAR N°1; 162 days for CAR N°4 and 139 days for CAR N°5) without any significant difference between the three CAR-T, although CAR N°1 and N°4 seemed better (Fig. 6D). Treatment with CAR-T slowed leukemic infiltration in the mice's blood compared to treatment with C0 (mean blasts at D38: C0: 352 blasts/µL; N°1: 201 blasts/µL; N°4: 160 blasts/µL and N°5: 240 blasts/µL), without significant difference, but with higher blast levels for CAR N°5 (Fig. 6E).

CAR N°1 is most effective in an aggressive BPDCN *in vivo* model

Considering the similar *in vivo* antitumor activity of CAR N°1 and N°4 in two BPDCN models, we aimed to discriminate them using the more aggressive BPDCN cell line Gen2.2, and to determine the differential phenotypic and transcriptomic profile between these two CAR-T (Fig. 7A**)**. At D0 we showed that PD-1 and LAG3 expression was higher on CAR N°4 than N°1 (PD1: 77.4% vs 62.8%; LAG3: 32.3 vs 19.1% respectively). No difference in TIM3 expression was noted (34.0% for CAR N°4 vs 35.7% for CAR N°1) (Fig. 7B). In contrast, the T-cell differentiation profile (T_{EFF}, T_{SCM}, T_{EM} and T_{CM}) of the two CAR-T did not differ significantly (Fig. 7C).

At the same time, CAR-T were sorted from mouse blood before performing a bulk RNA-sequencing analysis. We analyzed the differentially expressed genes between CAR N°1 and N°4 at D0 as well as CAR N°1 and CAR N°4 at D34. At D0, there was no difference in transcriptomic expression between CAR N°1 and N°4: only one gene (granulolysin/*GNLY*) was differentially expressed (Fig. 7D). At D34, of the 19,337 coding genes analyzed, only 160 had differential expression: 130 genes were down regulated and 30 were upregulated by CAR N°1 compared to N°4 (Fig. 7D **and Supplementary Table 3–4**). Among these genes, (*GNLY* and perforin/*PRF1*) and exhaustion genes (CTLA4/*CTLA4*, LAG3/*LAG3*, PD-1/*PDCD1*) were upregulated by CAR N°1 while the granzyme isoforms (*GZMA* and *GZMB*) and genes conferring a regulatory T profile (CD25/*IL2RA*, CCR4/*CCR4*, CCR8/*CCR8*) were down-regulated (Fig. 7E). Together, RNA sequencing showed that CAR N°1 and N°4 are not very different but CAR N°1 appears to have a less T-regulatory signature and more signs of cytotoxicity and exhausted profile at D34. Both CAR-T significantly limit circulation of BPDCN cells in mice until D34 (Fig. 7F) and both of them expand, thus exerting a significant anti-leukemic effect (Fig. 7F). CAR N°1 and N°4 significantly prolonged the survival of the mice (C0: 17 days, N°1: 90 days, N°4: 64 days) but among them, the CAR N°1 yielded the best results (Fig. 7G).

Discussion

BPDCN is a rare and aggressive hematological disease with very poor prognosis [2], and therapeutic strategies remain unconvincing. Advances in diagnostics and patient monitoring have shown that CD123-targeted approaches can be effective in treating this disease [41]. The first anti-CD123 approach developed for the treatment of BPDCN is a recombinant human interleukin-3 fused to a truncated diphtheria toxin (Tagraxofusp) [42], which obtained FDA approval for BPDCN treatment, but does not make it possible to avoid hematopoietic stem cell allograft [43, 44] and resistance [45, 46].

We sought to target CD123 for BPDCN treatment, since in our French cohort of 254 BPDCN cases, all cases expressed CD123 at high levels, on 100% of the blastic population [47], revealing CD123 as a promising TAA (Tumor Associated Antigens). Nevertheless, CD123 is not exclusively expressed by leukemic cells, since, importantly, a fraction of HSC, monocytes and endothelial cells expressed a low level of CD123. Nevertheless, it is essential to evaluate whether this low level can lead to destruction of these cells by CD123 CAR-T, and whether - depending of the scFv of CAR-T - there is a greater or lesser impact on $CD123^{low}$ positive cells.

The objective of our study was to choose the best scFv, inducing high functional effects on leukemic cells and sparing normal cells, to reduce the on-target/off-tumor effects. To this end, we developed five third-generation CAR-T (CD28/4-1BB/CD3ζ) targeting CD123 by substituting five different scFv.

We obtained high (> 96%) and stable transduction (until D23) for four CAR-T among the five. These four CAR-T activated nearly the same level of degranulation (CD107a) and cytokine secretion (IFN-γ/TNF-α) after contact with CAL-1 cell line. However, using unfavorable E:T ratios for co-culture, we show that CAR N°1, N°4 and N°5 are more functional than CAR N°2 and N°3. Moreover, *in vivo*, in two cell line-based BPDCN models and a PDX model, we show that CAR-T significantly reduce the tumor burden and the number of blasts in the blood, and significantly increase the median survival of mice with some variability between them.

To try to understand the differences induced by scFv substitution, we performed bulk RNA sequencing analysis on the two best CAR-T (N°1 and N°4) at D0 (final T-cell product) and at D34 after injection in a xenograft preclinical model. Bulk RNA sequencing analysis confirmed that there is nearly no difference between the two CAR-T at D0 whereas, after injection into mice and activation by the target cells (Gen2.2), there are slight differences between them (D34). CAR N°1 appears to have a less T-regulatory signature and more signs of cytotoxicity and T-cell exhaustion profile.

scFv are the most commonly used ligand-binding domains in the CAR-T construct. Many critical design parameters of the ligand-binding domain including affinity, avidity, antigen epitope location, and accessibility, could affect CAR-T functionality. Our five CAR-T were derived from five antibodies with high affinity for the antigen (ranging from 10^{-9}M to > 10^{-12}M). Such high affinities could induce targeting of healthy cells by these CAR-T, even if they present low CD123 expression. Therefore, it is necessary to determine the cytotoxicity of the four CAR-T against normal cells. Although CD123 expression remains limited on bone marrow HSC, hematotoxicity may be an obstacle to clinical development. Among the five CAR-T produced, two of them (N°3 and N°5) seem to induce higher cytotoxicity on autologous HSC, underlining that these two might induce higher hematotoxicity in patients. These findings could explain the contradictory data obtained in the literature concerning the toxicity of CD123 CAR-T [27–30, 48, 49] that have different scFv and backbone construction, highlighting the value of verifying this point before moving forward with clinical development.

Indeed, we show that CAR-T activation is weak against monocytes or endothelial cells, but not negative (higher than with $CD123^-$ Daudi cell line), suggesting that the activation of CAR-T remains moderate against healthy cells that weakly express CD123 but might be evaluated. Moreover, we highlight that cytokine production by activated CAR-T induced an increase (nearly twofold) in CD123 expression on endothelial cells, directly related to previously published data [31, 32]. We confirm secretion of IFN-γ and TNF-α by CAR-T after contact with a BPDCN cell line and a reversible increase of CD123 on endothelial cells during their exposure to these cytokines. However, we demonstrate low delayed toxicity of CAR-T using a real-time microscopy lysis assay during the first few hours of contact. These data highlight that

the potential endothelial toxicity of CAR-T might be low and could be controlled if necessary using pharmacological agents that inhibit IFN-γ or TNF-α (such as corticoids or adalimumab).

Controlling CAR-T for adverse toxicities is paramount, and thus, some studies have evaluated the addition of a suicide gene to make CAR-T sensitive to a drug that is very effective but irreversible for CAR-T [48–50]. More interestingly, reversible approaches are currently being evaluated to offer safety without inducing CAR-T elimination. The use of dasatinib, a tyrosine kinase inhibitor, can interrupt the activity of CAR-T (personal results not shown) in the event of unwanted toxicity, but without eliminating them [51–53]. Moreover, reducing CAR-T activation in this way might be useful to reduce induction of CD123 expression on endothelial cells.

In conclusion, we generated five CAR-T with different scFv, and show that the functionality of these CAR-T is different in terms of some key features, such as transduction efficacy, cytotoxic effect against normal cells and leukemic cells. Two of them have a better profile, with high cytotoxicity against BPDCN cells without high on-target/off-tumor effects. Particularly CAR N°1 shows significant, high intensity of CAR expression at the membrane, high cytotoxicity and activation against leukemic cells, and high benefit on mice survival without inducing high level of toxicity against normal cells. So, our study highlights the importance of evaluating various scFv in the context of building a new CAR-T.

Abbreviations

BPDCN: Blastic Plasmacytoid Dendritic Cell Neoplasm ; scFv: single chain Fragment variable ; CAR-T: Chimeric Antigen Receptor-T ; HSC: Hematopoetic Stem Cell ; CFU-GM: Colony Forming Unit-Granulocytes and Macrophages ; pDC: plasmacytoid dendritic cell ; HCT: hematopoietic cell transplantation ; mAb: monoclonal Antibody ; AML: Acute Myeloid Leukemia ; ALL: Acute Lymphoblastique Leukemia ; MDS: MyeloDysplastic Syndrome ; PDX: Patient Derived Xenograft ; PBMC: Peripheral Blood Mononuclear Cells ; MOI: Multiplicity of Infection ; FC: Flow cytometry ; LDH: Lactate DesHydrogenase ; TAA: Tumor Associated Antigens ; TNF-α: Tumor Necrosis Factor-α ; IFN-γ: Interferon-γ.

Declarations

Ethics approval and consent to participate

Collection of human peripheral blood mononuclear cells (PBMC) were obtained from healthy donors and patients after informed consent on protocols approved by the Etablissement Français du Sang (EFS) at Besançon. Mice were housed and treated in accordance with Animalerie Centrale/ UFR Santé UBFC/FC-EA481 and Ministère de la recherche (2021-004-OA-12PR).

Consent for publication

Not applicable

Competing interests

The authors declare no competing financial interests.

Funding

This study was supported by Programme de Recherche Translationnelle INCa (PRTK N°PRT-K-15-175), by the MiMedI project funded by BPI France (grant No.DOS0060162/00) and the European Union through the European Regional Development Fund of the Region Bourgogne-Franche-Comté (grant No. FC0013440) and by Association Laurette Fugain (ALF 2021/09).

Author's contributions

FGO, JG, OA, EBR, MF concept the project. FGO and JG supervised all the research. MF, MP, SB performed experiments. MF analysed data. RB. performed the bulk RNA-sequencing and E.S, MF and FR analysed these data. MF and EBR performed the lentivirus. FA, JC, ML, FB provided guidance and expertise in their respective areas of study. MF, FGO and JG wrote the manuscript and FD, PS, XR, Er D, Et D commented on the manuscript. All authors provided input, edited and approved the final version of the manuscript. The authors declare no conflict of interest.

Acknowledgments

The authors would like to thank Fiona Ecarnot, PhD, for English proofreading, Diaclone for collaboration for antibodies production, DImaCell Imaging Platform, the Laboratory of immunology (Jean Luc Poyard, Leila El Asraoui, Joelle Pariset, Thomas Fournet, Anne Roggy), the French BPDCN network (ROMI), the French Group of Cellular Haematology (GFHC) and the French Society of Haematology (SFH).

References

1. Kameoka J, Ichinohasama R, Tanaka M, Miura I, Tomiya Y, Takahashi S, et al. A Cutaneous Agranular CD2 $^{-}$ CD4 $^{+}$ CD56 $^{+}$ "Lymphoma": Report of Two Cases and Review of the Literature. Am J Clin Pathol. 1998;110:478–88.
2. Chaperot L. Identification of a leukemic counterpart of the plasmacytoid dendritic cells. Blood. 2001;97:3210–7.
3. Gruson B, Vaida I, Merlusca L, Charbonnier A, Parcelier A, Damaj G, et al. L-asparaginase with methotrexate and dexamethasone is an effective treatment combination in blastic plasmacytoid dendritic cell neoplasm. Br J Haematol. 2013;163:543–5.
4. Roos-Weil D, Dietrich S, Boumendil A, Polge E, Bron D, Carreras E, et al. Stem cell transplantation can provide durable disease control in blastic plasmacytoid dendritic cell neoplasm: a retrospective study from the European Group for Blood and Marrow Transplantation. Blood. 2013;121:440–6.
5. Dalle S, Beylot-Barry M, Bagot M, Lipsker D, Machet L, Joly P, et al. Blastic plasmacytoid dendritic cell neoplasm: is transplantation the treatment of choice?: BPDCN: is transplantation the treatment of

choice? Br J Dermatol. 2010;162:74–9.

6. Sadelain M, Brentjens R, Rivière I. The Basic Principles of Chimeric Antigen Receptor Design. Cancer Discov. 2013;3:388–98.
7. June CH, O'Connor RS, Kawalekar OU, Ghassemi S, Milone MC. CAR T cell immunotherapy for human cancer. Science. 2018;359:1361–5.
8. Hanssens H, Meeus F, De Veirman K, Breckpot K, Devoogdt N. The antigen-binding moiety in the driver's seat of CARs. Med Res Rev. 2021;med.21818.
9. Fujiwara K, Masutani M, Tachibana M, Okada N. Impact of scFv structure in chimeric antigen receptor on receptor expression efficiency and antigen recognition properties. Biochem Biophys Res Commun. 2020;527:350–7.
10. Zhang A, Sun Y, Du J, Dong Y, Pang H, Ma L, et al. Reducing Hinge Flexibility of CAR-T Cells Prolongs Survival In Vivo With Low Cytokines Release. Front Immunol. 2021;12:724211.
11. Qin L, Lai Y, Zhao R, Wei X, Weng J, Lai P, et al. Incorporation of a hinge domain improves the expansion of chimeric antigen receptor T cells. J Hematol OncolJ Hematol Oncol. 2017;10:68.
12. Hudecek M, Sommermeyer D, Kosasih PL, Silva-Benedict A, Liu L, Rader C, et al. The Nonsignaling Extracellular Spacer Domain of Chimeric Antigen Receptors Is Decisive for *In Vivo* Antitumor Activity. Cancer Immunol Res. 2015;3:125–35.
13. Almåsbak H, Walseng E, Kristian A, Myhre MR, Suso EM, Munthe LA, et al. Inclusion of an IgG1-Fc spacer abrogates efficacy of CD19 CAR T cells in a xenograft mouse model. Gene Ther. 2015;22:391–403.
14. Bras AE, Haas V, Stigt A, Jongen-Lavrencic M, Beverloo HB, Marvelde JG, et al. CD123 expression levels in 846 acute leukemia patients based on standardized immunophenotyping. Cytometry B Clin Cytom. 2019;96:134–42.
15. Taussig DC. Hematopoietic stem cells express multiple myeloid markers: implications for the origin and targeted therapy of acute myeloid leukemia. Blood. 2005;106:4086–92.
16. Huang S, Chen Z, Yu JF, Young D, Bashey A, Ho AD, et al. Correlation Between IL-3 Receptor Expression and Growth Potential of Human CD34 $^{+}$ Hematopoietic Cells from Different Tissues. STEM CELLS. 1999;17:265–72.
17. Sato N, Caux C, Kitamura T, Watanabe Y, Arai K, Banchereau J, et al. Expression and factor-dependent modulation of the interleukin-3 receptor subunits on human hematopoietic cells. Blood. 1993;82:752–61.
18. Brizzi MF, Garbarino G, Rossi PR, Pagliardi GL, Arduino C, Avanzi GC, et al. Interleukin 3 stimulates proliferation and triggers endothelial-leukocyte adhesion molecule 1 gene activation of human endothelial cells. J Clin Invest. 1993;91:2887–92.
19. Testa U, Riccioni R, Militi S, Coccia E, Stellacci E, Samoggia P, et al. Elevated expression of IL-3Rα in acute myelogenous leukemia is associated with enhanced blast proliferation, increased cellularity, and poor prognosis. Blood. 2002;100:2980–8.

20. Muñoz L, Nomdedéu JF, López O, Carnicer MJ, Bellido M, Aventín A, et al. Interleukin-3 receptor alpha chain (CD123) is widely expressed in hematologic malignancies. Haematologica. 2001;86:1261–9.
21. Fromm JR. Flow cytometric analysis of CD123 is useful for immunophenotyping classical Hodgkin lymphoma. Cytometry B Clin Cytom. 2011;80B:91–9.
22. Li LJ, Tao JL, Fu R, Wang HQ, Jiang HJ, Yue LZ, et al. Increased CD34 + CD38 – CD123 + cells in myelodysplastic syndrome displaying malignant features similar to those in AML. Int J Hematol. 2014;100:60–9.
23. DiPippo AJ, Wilson NR, Pemmaraju N. Targeting CD123 in BPDCN: an emerging field. Expert Rev Hematol. 2021;1–12.
24. Aldoss I, Clark M, Song JY, Pullarkat V. Targeting the alpha subunit of IL-3 receptor (CD123) in patients with acute leukemia. Hum Vaccines Immunother. 2020;16:2341–8.
25. Angelova E, Audette C, Kovtun Y, Daver N, Wang SA, Pierce S, et al. CD123 expression patterns and selective targeting with a CD123-targeted antibody-drug conjugate (IMGN632) in acute lymphoblastic leukemia. Haematologica. 2019;104:749–55.
26. Mardiros A, Dos Santos C, McDonald T, Brown CE, Wang X, Budde LE, et al. T cells expressing CD123-specific chimeric antigen receptors exhibit specific cytolytic effector functions and antitumor effects against human acute myeloid leukemia. Blood. 2013;122:3138–48.
27. Gill S, Tasian SK, Ruella M, Shestova O, Li Y, Porter DL, et al. Preclinical targeting of human acute myeloid leukemia and myeloablation using chimeric antigen receptor–modified T cells. Blood. 2014;123:2343–54.
28. Stevens BM, Zhang W, Pollyea DA, Winters A, Gutman J, Smith C, et al. CD123 CAR T cells for the treatment of myelodysplastic syndrome. Exp Hematol. 2019;74:52–63.e3.
29. Bôle-Richard E, Fredon M, Biichlé S, Anna F, Certoux J-M, Renosi F, et al. CD28/4-1BB CD123 CAR T cells in blastic plasmacytoid dendritic cell neoplasm. Leukemia. 2020;34:3228–41.
30. Tettamanti S, Marin V, Pizzitola I, Magnani CF, Giordano Attianese GMP, Cribioli E, et al. Targeting of acute myeloid leukaemia by cytokine-induced killer cells redirected with a novel CD123-specific chimeric antigen receptor. Br J Haematol. 2013;161:389–401.
31. Sun Y, Wang S, Zhao L, Zhang B, Chen H. IFN-γ and TNF-α aggravate endothelial damage caused by CD123-targeted CAR T cell. OncoTargets Ther. 2019;Volume 12:4907–25.
32. Chen Y, Li R, Shang S, Yang X, Li L, Wang W, et al. Therapeutic Potential of TNFα and IL1β Blockade for CRS/ICANS in CAR-T Therapy via Ameliorating Endothelial Activation. Front Immunol. 2021;12:623610.
33. Watanabe K, Terakura S, Martens AC, van Meerten T, Uchiyama S, Imai M, et al. Target Antigen Density Governs the Efficacy of Anti–CD20-CD28-CD3 ζ Chimeric Antigen Receptor–Modified Effector CD8 $^{+}$ T Cells. J Immunol. 2015;194:911–20.
34. Arcangeli S, Rotiroti MC, Bardelli M, Simonelli L, Magnani CF, Biondi A, et al. Balance of Anti-CD123 Chimeric Antigen Receptor Binding Affinity and Density for the Targeting of Acute Myeloid Leukemia.

Mol Ther. 2017;25:1933–45.

35. Alabanza L, Pegues M, Geldres C, Shi V, Wiltzius JJW, Sievers SA, et al. Function of Novel Anti-CD19 Chimeric Antigen Receptors with Human Variable Regions Is Affected by Hinge and Transmembrane Domains. Mol Ther. 2017;25:2452–65.
36. Krokhotin A, Du H, Hirabayashi K, Popov K, Kurokawa T, Wan X, et al. Computationally Guided Design of Single-Chain Variable Fragment Improves Specificity of Chimeric Antigen Receptors. Mol Ther - Oncolytics. 2019;15:30–7.
37. Anna F, Bole-Richard E, Fredon M, Certoux J-M, Souque P, Garnache-Ottou F, et al. Promoter's Choice Drive CAR-T Efficiency. J Biotechnol Biomed [Internet]. 2021 [cited 2021 Dec 6];04. Available from: https://www.fortunejournals.com/articles/promoterrsquos-choice-drive-cart-efficiency.html
38. Dobin A, Davis CA, Schlesinger F, Drenkow J, Zaleski C, Jha S, et al. STAR: ultrafast universal RNA-seq aligner. Bioinformatics. 2013;29:15–21.
39. Liao Y, Smyth GK, Shi W. featureCounts: an efficient general purpose program for assigning sequence reads to genomic features. Bioinformatics. 2014;30:923–30.
40. Love MI, Huber W, Anders S. Moderated estimation of fold change and dispersion for RNA-seq data with DESeq2. Genome Biol. 2014;15:550.
41. Shi M, Su RJ, Parmar K-P, Chaudhry R, Sun K, Rao J, et al. CD123: A Novel Biomarker for Diagnosis and Treatment of Leukemia. Cardiovasc Hematol Disord-Drug Targets. 2019;19:195–204.
42. Angelot-Delettre F, Roggy A, Frankel AE, Lamarthee B, Seilles E, Biichle S, et al. In vivo and in vitro sensitivity of blastic plasmacytoid dendritic cell neoplasm to SL-401, an interleukin-3 receptor targeted biologic agent. Haematologica. 2015;100:223–30.
43. Gourd E. Promising results with tagraxofusp in BPDCN. Lancet Oncol. 2019;20:e295.
44. Pemmaraju N, Lane AA, Sweet KL, Stein AS, Vasu S, Blum W, et al. Tagraxofusp in Blastic Plasmacytoid Dendritic-Cell Neoplasm. N Engl J Med. 2019;380:1628–37.
45. Alfayez M, Konopleva M, Pemmaraju N. Role of tagraxofusp in treating blastic plasmacytoid dendritic cell neoplasm (BPDCN). Expert Opin Biol Ther. 2020;20:115–23.
46. Stephansky J, Togami K, Ghandi M, Montero J, vonEgypt N, Lindsay R, et al. Resistance to SL-401 in AML and BPDCN Is Associated with Loss of the Diphthamide Synthesis Pathway Enzyme DPH1 and Is Reversible By Azacitidine. Blood. 2017;130:797–797.
47. Garnache-Ottou F, Vidal C, Biichlé S, Renosi F, Poret E, Pagadoy M, et al. How should we diagnose and treat blastic plasmacytoid dendritic cell neoplasm patients? Blood Adv. 2019;3:4238–51.
48. Cai T, Black KL, Naqvi A, Galetto R, Gouble A, Smith J, et al. Abstract 2560: Preclinical efficacy of allogeneic anti-CD123 CAR T-cells for the therapy of blastic plasmacytoid dendritic cell neoplasm (BPDCN). Immunology [Internet]. American Association for Cancer Research; 2018. p. 2560–2560. Available from: http://cancerres.aacrjournals.org/lookup/doi/10.1158/1538-7445.AM2018-2560
49. Zheng Y, Nandakumar KS, Cheng K. Optimization of CAR-T Cell-Based Therapies Using Small-Molecule-Based Safety Switches. J Med Chem. 2021;64:9577–91.

50. Warda W, Da Rocha MN, Trad R, Haderbache R, Salma Y, Bouquet L, et al. Overcoming target epitope masking resistance that can occur on low-antigen-expresser AML blasts after IL-1RAP chimeric antigen receptor T cell therapy using the inducible caspase 9 suicide gene safety switch. Cancer Gene Ther. 2021;28:1365–75.
51. Mestermann K, Giavridis T, Weber J, Rydzek J, Frenz S, Nerreter T, et al. The tyrosine kinase inhibitor dasatinib acts as a pharmacologic on/off switch for CAR T cells. Sci Transl Med. 2019;11:eaau5907.
52. Weber EW, Lynn RC, Sotillo E, Lattin J, Xu P, Mackall CL. Pharmacologic control of CAR-T cell function using dasatinib. Blood Adv. 2019;3:711–7.
53. Leclercq G, Haegel H, Schneider A, Giusti AM, Marrer-Berger E, Boetsch C, et al. Src/lck inhibitor dasatinib reversibly switches off cytokine release and T cell cytotoxicity following stimulation with T cell bispecific antibodies. J Immunother Cancer. 2021;9:e002582.
54. Philippe L, Ceroi A, Bôle-Richard E, Jenvrin A, Biichle S, Perrin S, et al. Bortezomib as a new therapeutic approach for blastic plasmacytoid dendritic cell neoplasm. Haematologica. 2017;102:1861–8.

Figures

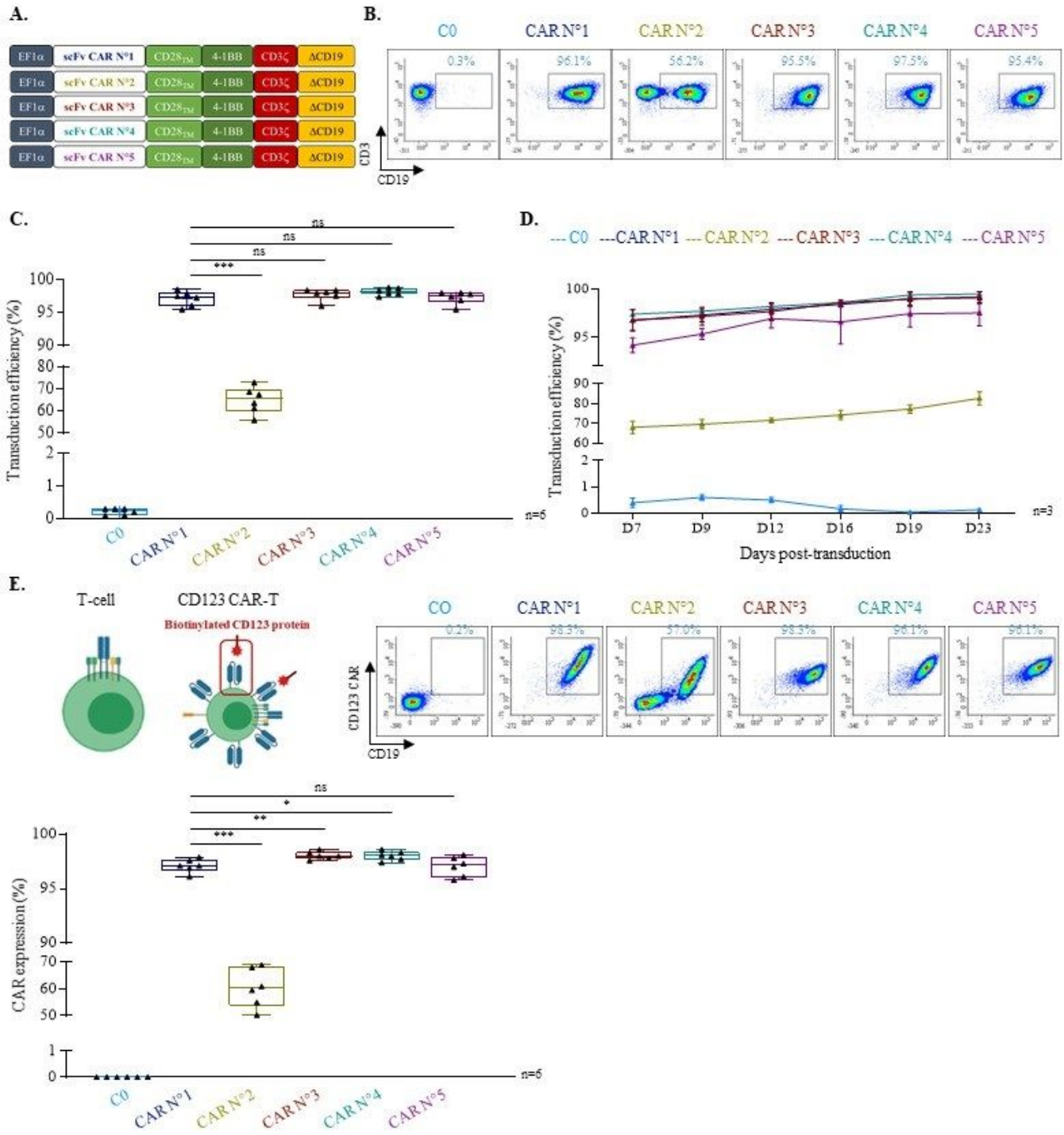

Figure 1

CD123 CAR-T design, transduction and expression. (A) Schematic diagram of five CD123 CAR-T composed of EF1a promotor, different CD123 scFv, CD28 and 4-1BB co-stimulation domains and selection marker (DCD19). (B)/(C) Transduction efficiency of CD123 CAR-T was measured by flow cytometry using CD3 and CD19 antibodies seven days after transduction. (D) Stability of transduction efficiency was evaluated by flow cytometry using CD3 and CD19 antibodies on day 7 to day 23-post

transduction. (E) CD123 CAR expressions was detected by flow cytometry using biotinylated CD123 protein on day 9 post transduction. Data presented are mean ± SD. C0, non-transduced T-cell; ns, not significant; 0.033 (*), 0.002 (**), <0.001 (***) compared to CAR N°1.

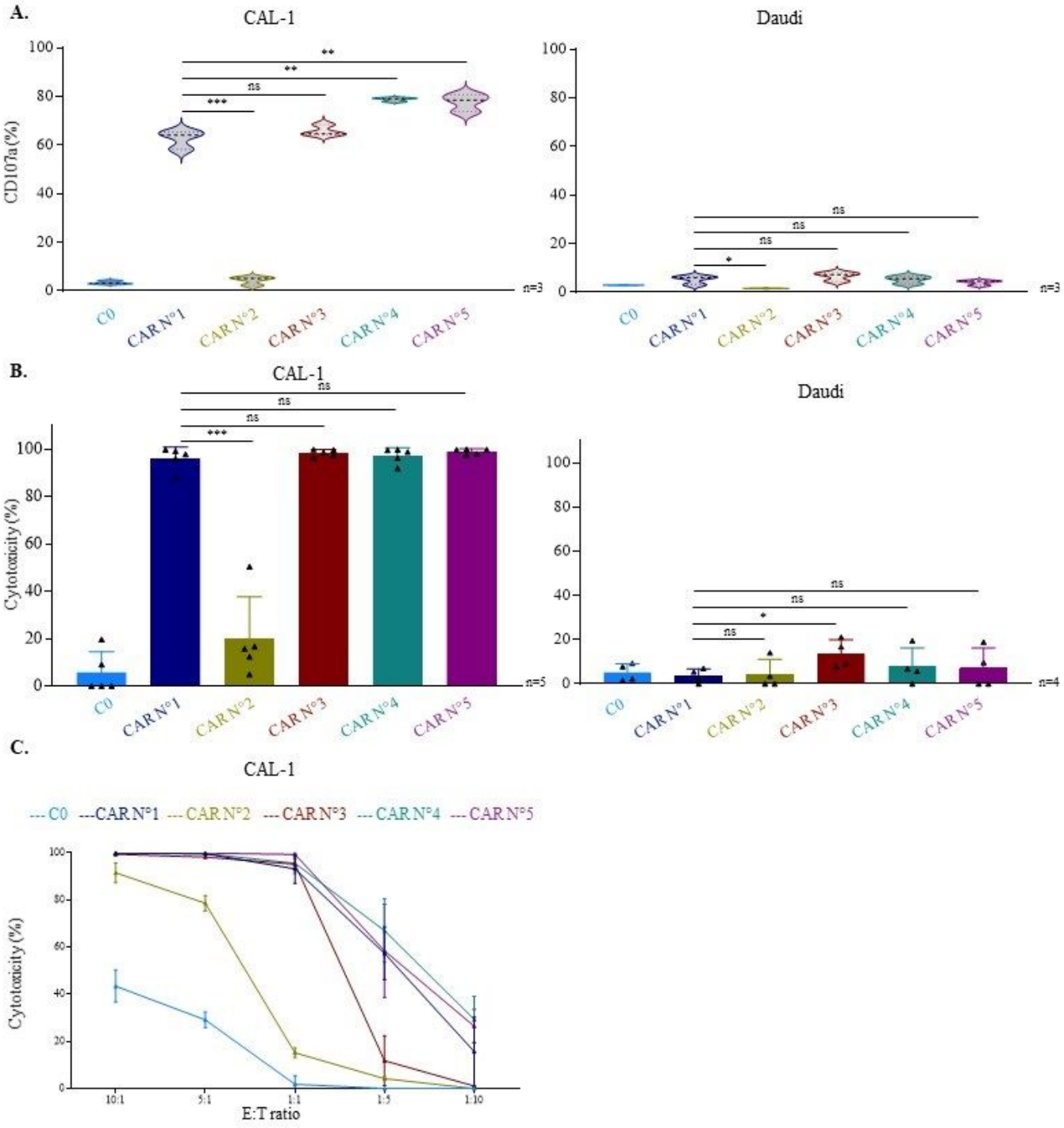

Figure 2

Anti leukemic activity of CD123 CAR-T is antigen specific. (A) CD107a expression of C0 or CD123 CAR-T after 6 hours of co-culture with target cells at an E: T ratio of 1:1 using flow cytometry. (B) Cell death of target cells was measured by flow cytometry using 7-AAD labelling. Effectors cells were labeled with eFluor before co-cultured with target cells at an E: T ratio of 1: 1 for 24 hours. (C) Cell death of CAL-1 cell line was measured by flow cytometry using 7-AAD labelling. Effector cells were labeled with eFluor before co-cultured with CAL-1 cell line at an E: T ratio of 10: 1; 5: 1; 1: 1; 1: 5 and 1: 10 for 24 hours. Data presented are mean ± SD. ns, not significant; 0.033 (*), 0.002 (**), <0.001 (***) compared to CAR N°1. E: T, Effector: Target.

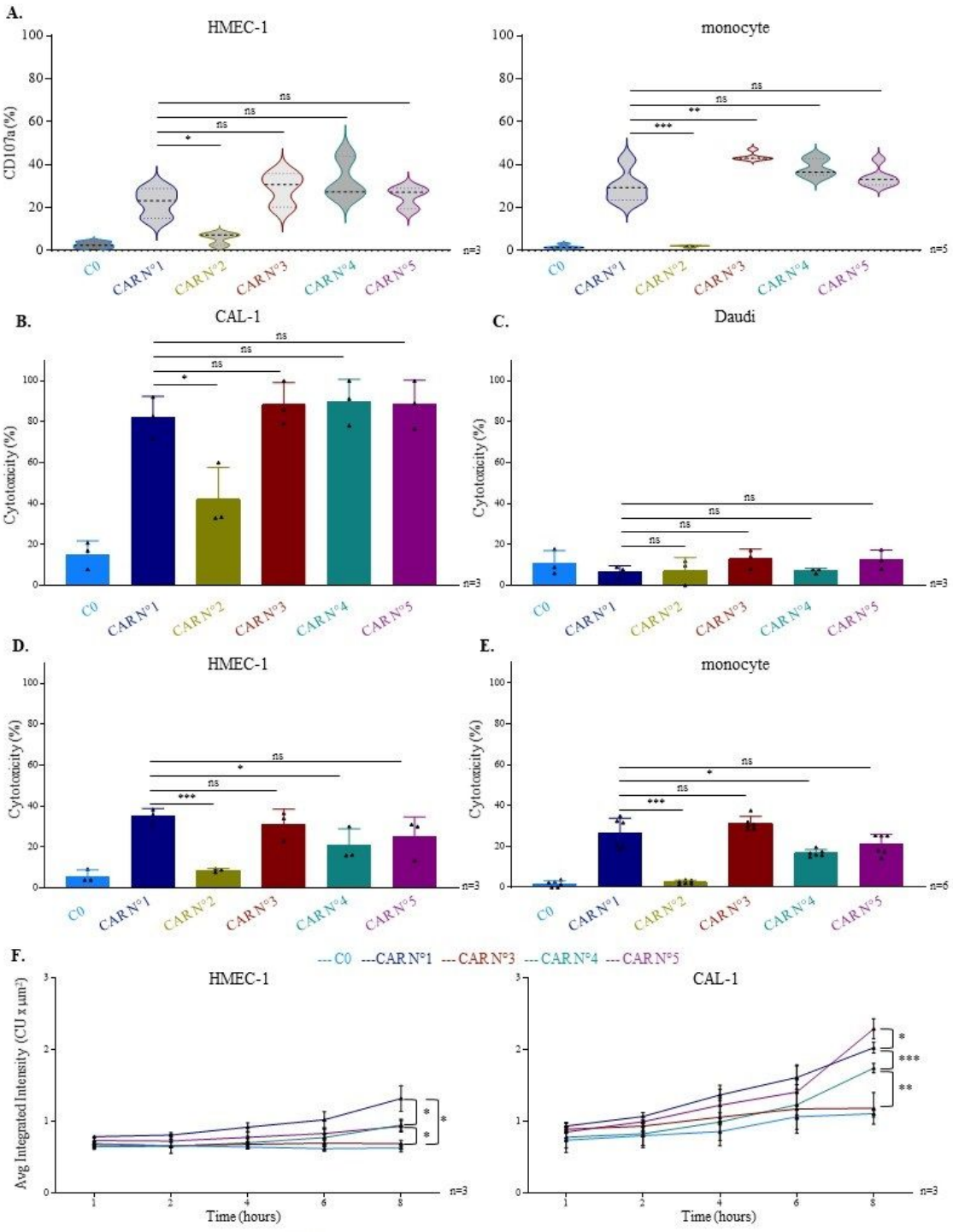

Figure 3

CD123 CAR-T have low impact on healthy cells. (A) CD107a expression of C0 or CD123 CAR-T after 6 hours of co-culture with endothelial cells or monocytes at an E: T ratio of 1:1 using flow cytometry. Cell death of (B) CAL-1, (C) Daudi, (D) HMEC-1 (E) and monocytes was evaluated by bioluminescence using the LDH release assay after 24 hours of co-culture at an E:T ratio of 1:1. (F) Real time killing of HMEC-1 (left) and CAL-1 (right) was followed by Incucyte ® (zoom x10, phase and green 400ms acquisition time,

1 scan every hour). HMEC-1 and CAL-1 were labeled with green apoptosis dye before co-culture. Data presented are mean ± SD. ns, not significant; 0.033 (*), 0.002 (**), <0.001 (***) compared to CAR N°1.

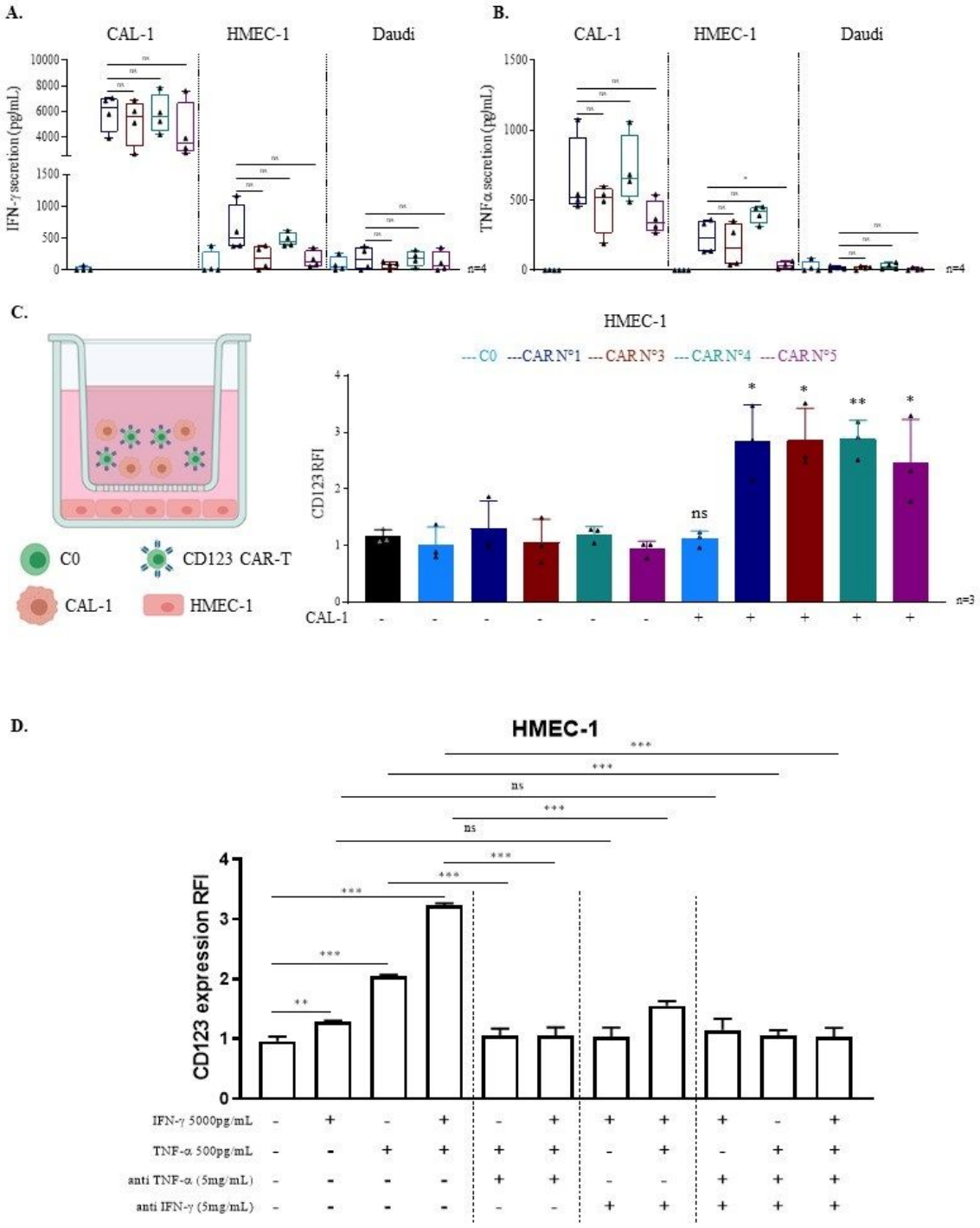

Figure 4

Impact of IFN-g and TNF-a on CD123 expression by endothelial cells. (A) IFN-g secretion was measured by ELISA in culture supernatants after 24 hours of co-culture between C0 or CD123 CAR-T and CAL-1 or

HMEC-1 or Daudi. (B) TNF-a secretion was measured by ELISA in culture supernatants after 24 hours of co-culture between C0 or CD123 CAR-T and CAL-1 or HMEC-1 or Daudi. (C) Schematic diagram of tri-culture model. Effector cells (C0 or CD123 CAR-T) and target cells (CAL-1) were seeded in the upper chamber at an E: T ratio of 1: 1 and HMEC-1 were placed in lower chamber. After 24 hours of co-culture, HMEC-1 were digested with trypsin to assess the CD123 expression by flow cytometry. Data presented are mean ± SD. ns: not significant; 0.033 (*), 0.002 (**), <0.001 (***).

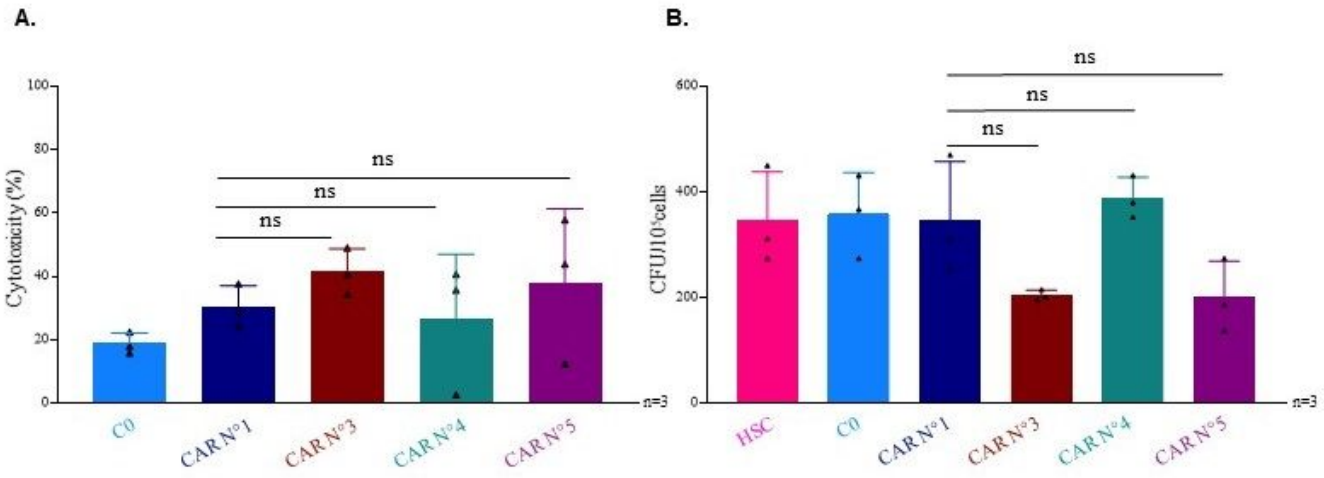

Figure 5

Autologous CD123 CAR-T do not affect hematopoietic stem cells. (A) HSC from cord blood were selected by CD34-immunomagnetic beads and co-cultured with autologous C0 or CD123 CAR-T at an E: T ratio of 1: 1 for 18 hours. Then we analysed cytotoxicity by flow cytometry. (B) After co-culture, one part of co-culture was plated in semisolid methylcellulose progenitor culture. After 14 days, the number of CFU was manually counted. Data presented are mean±SD. ns: no significant difference.

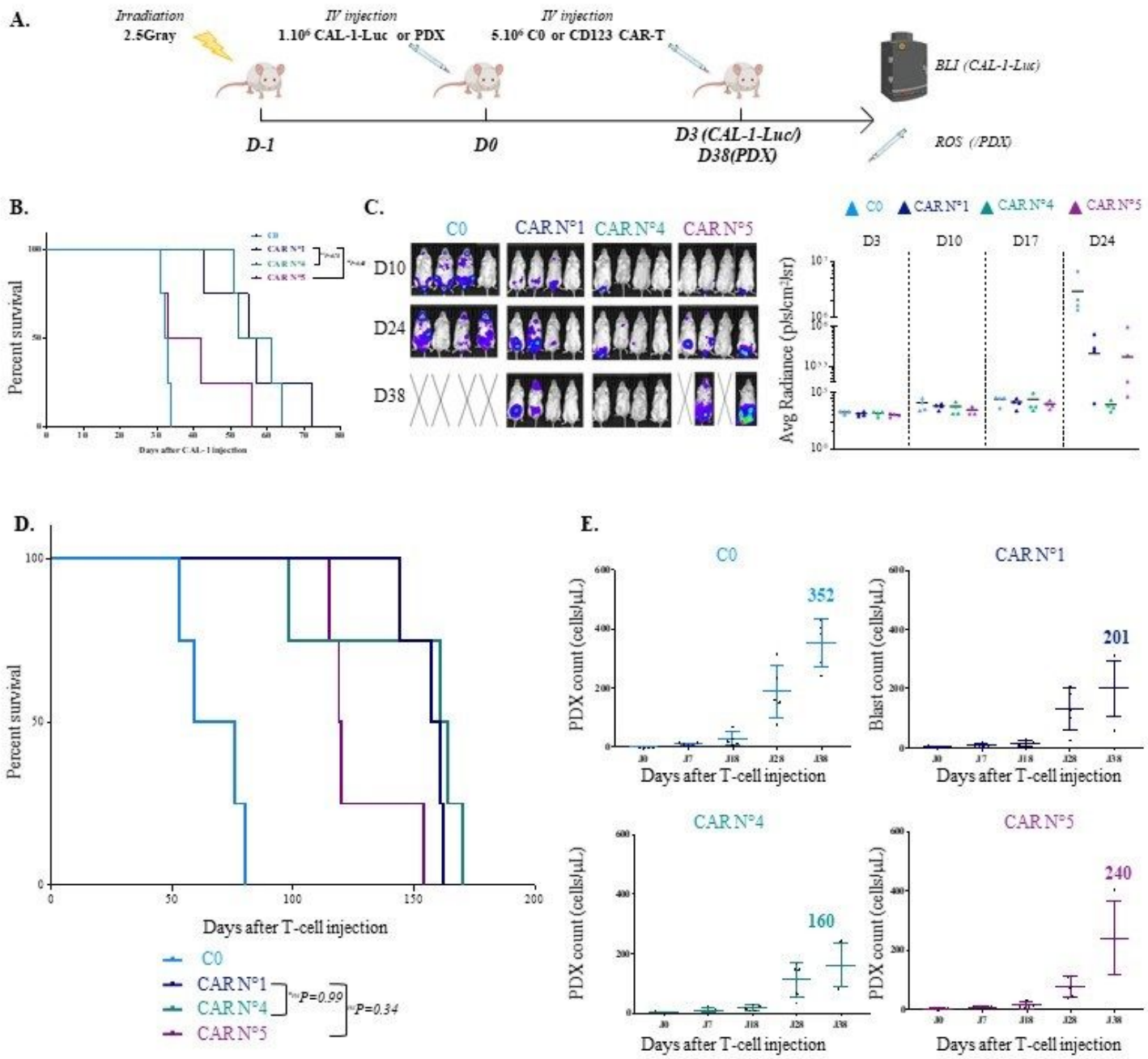

Figure 6

CD123 CAR-T reduce BPDCN growth *in vivo* (CAL-1-Luc/PDX/Gen2.2). (A) Schematic diagram of the xenograft model. (B) CAL-1-luc survival curve was analysed from CAL-1-Luc injection until the death. The general health of the mice was assessed during the experiment (data not shown). (C) Bioluminescence imaging analysis before and during C0 or CD123 CAR-T treatment up to 24 days after CAL-1-Luc injection. (D) PDX survival curve was analysed from C0 or CD123 CAR-T injection. (E) PDX cells from peripheral blood were analysed by flow cytometry.

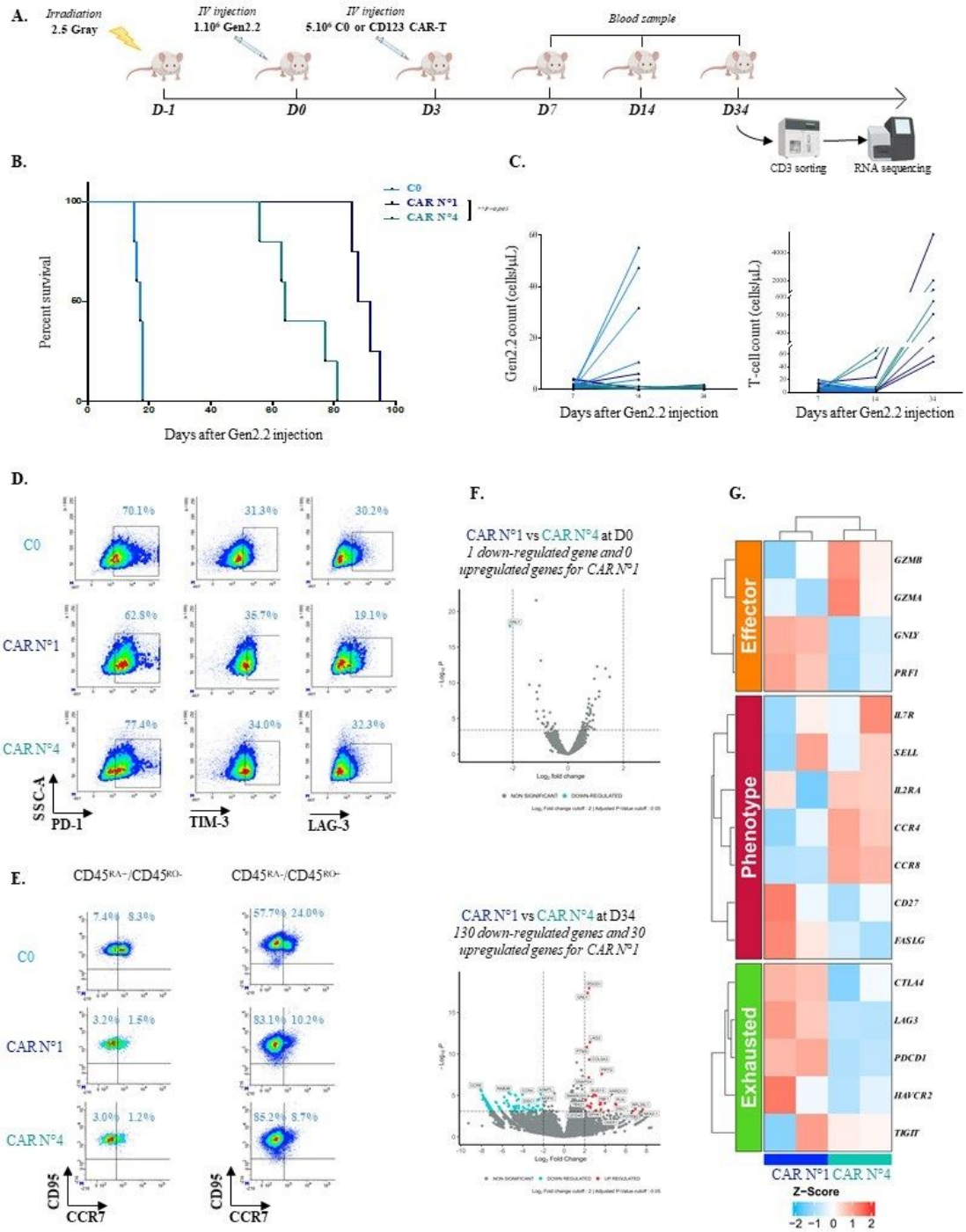

Figure 7

CAR N°1 most effective in an aggressive BPDCN *in vivo* model. (A) Schematic diagram of the xenograft model. CAR N°1 and N°4 were sorted from peripheral blood before being analysed by bulk RNA sequencing. (B) Mice survival curves were analysed for Gen2.2 model. (C) Gen2.2 cells or T-cell counts in mice blood. (D) Exhausted phenotype and (E) differentiation T-cell phenotype of C0. CAR N°1 and CAR N°4 at D0 (before injection). (F) Volcano plot showing differentially expressed genes in CAR N°1

compared to CAR N°4 at D0 and at D34. (G) Heatmap of normalized expression from bulk RNA-sequencing analysis of differential expression genes of CAR N°1 and CAR N°4 at D34.

Supplementary Files

This is a list of supplementary files associated with this preprint. Click to download.

- Supplemental.docx